# Hyperelastic nature of Hoek-Brown criterion

Ilaria Fontana, Kyrylo Kazymyrenko, Daniele Di Pietro

# Hyperelastic nature of Hoek–Brown criterion

Ilaria Fontana [*,1,2], Kyrylo Kazymyrenko[2], and Daniele A. Di Pietro[1]

[1]IMAG, Univ Montpellier, CNRS, Montpellier, France
[2]UMR EDF-CNRS-CEA-ENSTA 9219, IMSIA, Palaiseau, France

**Abstract**

We analyze the influence of hyperelasticity on the plastic behavior of materials. A specific class of what we call hyperbolic elasticity arises from theoretical considerations as straight consequence of plastic invariance of elastic domain. The latter property of fixed residual plasticity is observed experimentally for many geomaterials. We superimpose hyperelastic effects on the plastic Drucker–Prager constitutive relation, widely used in geoscience. Curiously, we found that the hyperbolic nonlinearity, introduced through the Standard Generalized Material formalism, curves the initially linear surface to a quadratic one, that is assimilated to the generalized Hoek–Brown criterion. We conclude than that one possible justification of the empirical Hoek–Brown fit is the material's hyperlastic nature.

**Keywords:** hyperelasticity, elasto-plastic model, Hoek–Brown criterion, constitutive relation, Drucker–Prager criterion, Fairhurst criterion

## 1 Introduction

One of the key points in the accurate description of rocks is the precise identification of their elastic domain (or yield surface/criterion). Due to the softening behavior, not only rocks but also all analogous materials like concrete, clay, soil or even ice [33] are commonly classified by their resistance to various mixed mode loading. This approach is closely related to the basic safety rules in industrial applications, where it is often considered that geomaterials could exhibit unstable failure once the critical loading is reached [14].

Throughout the last century, specific testing machines and corresponding measurement protocols were established by national and international committees in order to harmonize and standardize the experimental characterization of the above-cited brittle materials. To mention only a few, the brazilian tensile [3], oedometric, uni- and tri-axial compression are all well documented experiments that are routinely executed to catalog material strength by spotting just some points of their multidimensional yield surface. This reduced "single point" vision of material resistance is increasingly scrutinized in recent times, and multiple evolutions have been adopted. For instance, constant improvements of finite element software enable new kinds of modeling, with loadings going beyond the elastic domain to explore a more subtle post-peak behavior. In the corresponding mechanical tests, the response of the material subjected to a set of pre-established loadings is analyzed during both the elastic and softening phase, enabling the full model parameter fitting. Some

*Corresponding author

more sophisticated hybrid measurement techniques are also proposed, where the loading pass is adapted during the test execution. A single, all in one experiment, replaces the classical set with the same goal of full model identification [18]. While the complexity of post-peak description could be reached through various theoretical formalisms, most of them still rely on the initial yield surface definition, and the question of this elastic domain shape remains the cornerstone of any non-linear model identification. Even if considerable progress was made in recent decades, this precise identification of yield surface remains nowadays a rather challenging task [21].

A common feature of geomaterials is their strong resistance to compressive loading. For some large scale structures, like hydraulic dams or underground tunnel excavations, the construction material is naturally submitted to high levels of compression. For others, like nuclear confinement buildings or bridges, civil engineering constitutive concrete parts are pre-loaded to reach artificially an initial compression state by supplementary constraint of tension reinforcing steel tendons. In both cases, the property of higher compressive resistance is exploited on industrial level with the aim of increasing global structure robustness.

According to the physical origin of geomaterials, a large variety of criteria defining the elastic domain are employed in order to model their mechanical behavior. The simplest surface, admitting infinite resistance in compression, is the linear cone-shaped one. It was first introduced more than a century ago and, depending on whether it is written in principal stresses or with help of rotational invariants, it's commonly called either Mohr–Coulomb [4, 25] or Drucker–Prager [6] criterion. Straight relation between shear and compressive loadings, which is the main signature of these linear criteria, has allowed the development of various constitutive relations based on the same simplified dependence [20, 1].

In the middle of the last century, with numerous large infrastructural projects ongoing, more complex criteria emerged as further experimental data became available. For wider ranges of loadings, the friction-type shear dependency seemed to be deflecting from the linear curve. Logically, a quadratic relation was to be explored first. Back in 1924, assuming the hypothesis of crack propagation via rapid growth of randomly distributed micro-flaws, Griffith had already obtained a theoretical justification of the parabolic yield shape [10]. Inspired by the Griffith's model, Fairhust proposed its empirical extension validated on the tensile Brazilian test [9]. In this spirit, in 1980 Evert Hoek and Edwin T. Brown [13] came up with a new particular shape of quadratic nonlinear criterion. It reproduced the Mohr–Coulomb type singularity for weak tensile loading simultaneously taking into account the reduction of shear resistance for high compression. Purely empirical, the Hoek–Brown criterion was originally obtained for intact rocks by two parameters fitting of the results of triaxial tests. Validated during the following years on wider experimental database, the criterion was used extensively in the design of underground excavations [14].

It should be underlined that not only previously cited [10, 9, 13], but many other authors (e.g. [28]) kept the number of model parameters reduced, so that the better fit was obtained by the new curve's form itself, rather then by the addition of supplementary fitting variables. Consequently, the final expression of the failure criteria, being pure result of trial error process, appears quite artificial at first glance. *In this article we try to establish a possible hyperelastic link between the whole class of quadratic Hoek–Brown type criteria and their linear Mohr–Coulomb (Drucker–Prager) counterparts.* The single hypothesis of existence of a stable failure surface under free-energy type description generates a sub-class of quadratic yield surfaces from the linear relation of generalized

plastic force. The Hoek–Brown relation is seen then as a consequence of the simultaneous presence of both plasticity and nonlinear elasticity phenomena in the geomaterial under investigation.

## 2 Main idea in the nutshell

In this section we summarize the main idea of the article reducing as far as possible technical details and complex notation that are required for a rigorous theoretical description.

Under the small deformation hypothesis, the thermodynamical description of continuum mechanics relies on the Helmholtz free energy density definition. For isothermal evolution in presence of plasticity, this function depends on at least two state variables: the total strain $\boldsymbol{\varepsilon}$ and the plastic strain $\boldsymbol{p}$, i.e., $\phi(\boldsymbol{\varepsilon}, \boldsymbol{p})$. The Cauchy stress tensor is then the dual conjugate to the total strain $\boldsymbol{\sigma} = \partial\phi/\partial\boldsymbol{\varepsilon}$, while the energy response of the system on plastic strain evolution is captured through the generalized plastic force $\boldsymbol{X} = -\partial\phi/\partial\boldsymbol{p}$. Most elasto-plastic models admit additive separation of elastic and plastic strains. This leads to the simplest quadratic form of free energy describing residual plastic state :

$$\phi(\boldsymbol{\varepsilon}, \boldsymbol{p}) = \frac{1}{2}\mathbb{E}(\boldsymbol{\varepsilon} - \boldsymbol{p})^2, \tag{2.1}$$

where $\mathbb{E}$ is the constant elastic modulus. Notice that we adopt abridged notations for tensor operations. In particular, in this linear elastic case, the generalized plastic force and Cauchy stress are equal:

$$\boldsymbol{\sigma} = \boldsymbol{X} = \mathbb{E}(\boldsymbol{\varepsilon} - \boldsymbol{p}). \tag{2.2}$$

The reversible elastic domain, characterized by the absence of plasticity evolution, is defined in the space of generalized force: $\boldsymbol{p} = \text{const} \Rightarrow \boldsymbol{X} \in \mathbb{K}_{\boldsymbol{X}}$. As we have mentioned in the introduction, considerable experimental efforts are focused on the identification of the elastic domain. In perfect plasticity hypothesis, the domain is fixed during evolution and it could consequently be considered as main material property. On further stage of model development, a plastic variable evolution is introduced, as it is commonly done either trough dissipation potential [11], plastic potential [31] or directly via explicit flow rule. Among the many possible existing extensions of the basic perfect plasticity constitutive model, we focus this work on the modification of the shape of the elastic domain generated by hyperelasticity [27].

Unlike Cauchy elasticity, that postulates linear (Hooke's law) or non linear straight stress-strain relationship, hyperelasticity admits the existence of scalar strain energy density function from which the stress is derived: $\boldsymbol{\sigma} = \partial\phi/\partial\boldsymbol{\varepsilon}$. In this sense, the hyperelastic formalism is conservative and is compatible with a general thermodynamical description. Usually written for large strain [27], it is easily adapted to the small strain hypothesis [26].

Let us suppose that, in (2.1), the elastic modulus is some function of the total infinitesimal strain, i.e., $\mathbb{E} = \mathbb{E}(\boldsymbol{\varepsilon})$. The stress-strain relationship becomes nonlinear and the stress is no longer equal to the generalized plastic force:

$$\boldsymbol{X} = \mathbb{E}(\boldsymbol{\varepsilon} - \boldsymbol{p}) \neq \boldsymbol{\sigma}.$$

Formal writing of the expression for the stress gives:

$$\boldsymbol{\sigma} = \mathbb{E}(\boldsymbol{\varepsilon} - \boldsymbol{p}) + \frac{\partial\mathbb{E}}{2\partial\boldsymbol{\varepsilon}}(\boldsymbol{\varepsilon} - \boldsymbol{p})^2 = \boldsymbol{X} + \frac{\partial\mathbb{E}}{2\mathbb{E}^2\partial\boldsymbol{\varepsilon}}\boldsymbol{X}^2. \tag{2.3}$$

If the elastic domain is fixed in the space of generalized force $\boldsymbol{X}$, in the presence of hyperelasticity it becomes strain dependent in the space of stresses $\boldsymbol{\sigma}$: $\mathbb{K}_{\boldsymbol{\sigma}}$. For small loading ($\boldsymbol{X} \ll 1$) the quadratic term $\sim \boldsymbol{X}^2$ could be considered as a nonlinear cinematic hardening, but in general the equation (2.3) states the nonlinear modification of the initial elastic domain $\mathbb{K}_{\boldsymbol{\sigma}} \neq \mathbb{K}_{\boldsymbol{X}}$. For plastifying cyclic loading, the initial yield surface is modified on each back-and-forth loop creating a mechanism similar to those introduced earlier by different authors, like bounding surface in [5] or parent/child surfaces in Hujeux constitutive behaviour [2]. Therefore, the presence of hyperelasticity in plastic materials introduces not only a nonlinear stress-strain relationship, but also a modification of elastic domain represented in stress space.

Nonlinear behaviors of rocks, clays and soils are historically well known, but are often considered less relevant than other major mechanical phenomena, like fracture, plasticity, dilatancy etc. For most geomaterials the reversible elastic domain is comparatively small and hard to quantify experimentally. Nevertheless, some recent well documented experiments manage to separate and evaluate the elastic nonlinearity itself. For example, in [19] the authors conducted locally cyclic loadings on sand that revealed its hyperelastic properties. Even if this new experiment sheds light on this longtime forgotten phenomenon, the general hyperelastic coupling term is too complex to be fully identified. Natural question arise on how to handle all possible couplings in the multidimensional tensor relation $\mathbb{E}(\boldsymbol{\varepsilon})$. In this article, it is shown that hyperelastic coupling term can be simplified (2.4) enabling its analysis with the currently accessible experimental databases (e.g. [19]).

We introduce a particular class of hyperelasto-plastic materials that have fixed yield criterion in the stress space. This yield criterion can be considered either as initial elastic domain or as residual yield surface, for example for fully damaged elasto-plastic coupled to damage behavior [24]. As the elastic domain in the space of generalized force $\boldsymbol{X}$ is supposed to be fixed, it would also stay fixed in the space of stresses $\boldsymbol{\sigma}$ if and only if the coupling term in (2.3) is constant:

$$\frac{\partial \mathbb{E}}{2\mathbb{E}^2 \partial \boldsymbol{\varepsilon}} = \text{const}.$$

This condition defines one particular class of hyperelastic materials that keep the elastic domain fixed. This equation states that the material compliance should be linear with total strain:

$$\frac{\partial \mathbb{E}}{2\mathbb{E}^2 \partial \boldsymbol{\varepsilon}} = -\frac{\partial \mathbb{E}^{-1}}{2\partial \boldsymbol{\varepsilon}} = \text{const} \qquad \Longrightarrow \qquad \mathbb{E}^{-1} \sim \boldsymbol{\varepsilon}. \tag{2.4}$$

This formal writing of a tensor based expression is certainly over-simplified, but it allows us to propose a sub-class of hyperelastic materials that has fixed yield surface. For instance, we could reach this condition by setting both Lamé coefficients as hyperbolic functions of the strain trace. This particular case of hyperelasticity and subsequent constitutive relation obtained under the assumption of Standard Generalized Materials [11, 8] are analyzed in detail in the next section. In particular, we will show that the model constructed starting from a Drucker–Prager (linear) plasticity criterion in the generalized force space will lead to a nonlinear hyperelastic constitutive law with a quadratic Hoek–Brown type domain in the stress space.

## 3 Hyperelasticity with fixed plastic yield surface

Inspired by the ideas presented shortly above, in this section we display how to derive the elasto-plastic model with a three-dimensional Hoek–Brown–type yield criterion, adding a

specific type of hyperelasticity to the initially linear plasticity criterion.

Above and throughout this section, we use the usual notation of mechanics: $\boldsymbol{u}$ is the unknown displacement field, $\boldsymbol{\varepsilon} \in \mathbb{R}^{3\times3}_{\text{sym}}$ is the strain tensor, i.e., the symmetric part of the gradient of $\boldsymbol{u}$, $\boldsymbol{p} \in \mathbb{R}^{3\times3}_{\text{sym}}$ is the plasticity component of the strain tensor, i.e., $\boldsymbol{p} = \boldsymbol{\varepsilon} - \boldsymbol{\varepsilon}^{\text{el}}$, $\boldsymbol{\sigma} \in \mathbb{R}^{3\times3}_{\text{sym}}$ is the stress tensor, and $\boldsymbol{X} \in \mathbb{R}^{3\times3}_{\text{sym}}$ is the thermodynamical force associated with plasticity, i.e., the plastic dual variable. Strain and plasticity tensors are the state variables of our model and, for simplicity, they are decomposed into their volumetric and deviatoric parts:

$$\boldsymbol{\varepsilon} = \frac{1}{3}\mathrm{Tr}\,\boldsymbol{\varepsilon}\,\mathbf{I}_2 + \boldsymbol{\varepsilon}^D \qquad \text{and} \qquad \boldsymbol{p} = \frac{1}{3}\mathrm{Tr}\,\boldsymbol{p}\,\mathbf{I}_2 + \boldsymbol{p}^D.$$

We adopt the usual convention in mechanics of continuous media for the sign of strain and stress, i.e., the stress is positive in traction and negative in compression.

### 3.1 Brief history of quadratic yield criteria

We start first with a brief description of the history of the introduction of quadratic yield surfaces, what we call "Hoek–Brown–type" yield surfaces.

Back in 1924, while studying the mechanical behavior of glasses, Griffith [10] was the first to derive from theoretical considerations a quadratic multi-axial criterion for fracture:

$$(\sigma_1 - \sigma_3)^2 \sim (\sigma_1 + \sigma_3)$$

where $\sigma_1$ and $\sigma_3$ the major and minor principal stresses, respectively.

Forty years later, Fairhust [9] attempted to empirically extend the work of Griffith for the domain of high compression suitable for rock behavior analysis.

Finally, in 1980 Hoek and Brown [13] obtained a criterion shape that convinced many generations of geomaterial scientists. The original Hoek–Brown criterion is still widely used in rock mechanics and, for intact rocks, it can be written as:

$$\sigma_1 = \sigma_3 + C_0\sqrt{m_i\frac{\sigma_3}{C_0} + 1},$$

where $C_0$ is the uniaxial compressive strength and $m_i$ is a material constant for the intact rock. For more details about these constants, we refer to [15, 16], where a generalized version of the criterion involving the geological strength index (GSI) is also proposed and analyzed. Furthermore, the evolution of the Hoek–Brown criterion in the literature is summarized in the article [17].

Since many papers have exhibited the strong influence of the intermediate principal stress $\sigma_2$ (see, e.g., [22, 7] and the references therein), different three-dimensional extensions based on the Hoek–Brown criterion have been developed [29, 32, 30, 22]. In particular, the generalized form of the Pan–Hudson criterion proposed by X. D. Pan and J. Hudson [28] reads, for an intact rock, as :

$$\frac{3}{2C_0}\left\|\boldsymbol{\sigma}^D\right\|^2 + \frac{\sqrt{3}m_{\text{i}}}{2\sqrt{2}}\left\|\boldsymbol{\sigma}^D\right\| + m_{\text{i}}\sigma_m - C_0 = 0,$$

where $\sigma_m$ and $\boldsymbol{\sigma}^D$ are the spherical and deviatoric part of the stress tensor, respectively, i.e.,

$$\boldsymbol{\sigma} = \sigma_m\,\mathbf{I}_2 + \boldsymbol{\sigma}^D, \qquad \text{where } \sigma_m = \frac{1}{3}\mathrm{Tr}\,\boldsymbol{\sigma}, \tag{3.1}$$

and $\left\|\boldsymbol{\sigma}^D\right\| \coloneqq \sqrt{\boldsymbol{\sigma}^D : \boldsymbol{\sigma}^D}$. Here, $\mathbf{I}_2$ denotes the second order identity tensor, and the double dot product is simply the double contraction operation for second order tensors. All the described criteria are parabolic and can be summarized as various choices of constants in the general expression:

$$f_{\boldsymbol{\sigma}} = A\left\|\boldsymbol{\sigma}^D\right\|^2 + B\left\|\boldsymbol{\sigma}^D\right\| + C\sigma_m - D = 0.$$

In this article we don't suppose, but derive quadratic yield criterion of this type under the assumption of Standard Generalized Materials [11] in a variational framework in presence of hyperelasticity. In particular, as we have already mentioned, we will show that this model can be constructed by starting from and elasto-plastic model with a Drucker–Prager (linear) plasticity criterion and introducing hyperbolic hyperelastic dependence in some material parameters. This will lead to a nonlinear elastic constitutive relation with Hoek–Brown type yield surface.

### 3.2 Energy density and derivation of the stress tensor

We begin our analysis by precising the tensor notation for the perfect elasto-plastic model already introduced in the previous section. In particular, the considered free energy density corresponds to the non-hardening version of [24, Equation (11)], where the material is assumed to be isotropic:

$$\begin{aligned}\phi(\boldsymbol{\varepsilon}, \boldsymbol{p}) &= \frac{1}{2}\mathbb{E}(\boldsymbol{\varepsilon} - \boldsymbol{p}) : (\boldsymbol{\varepsilon} - \boldsymbol{p}) \\ &= \frac{1}{2}K(\operatorname{Tr}\boldsymbol{\varepsilon} - \operatorname{Tr}\boldsymbol{p})^2 + \mu(\boldsymbol{\varepsilon}^D - \boldsymbol{p}^D) : (\boldsymbol{\varepsilon}^D - \boldsymbol{p}^D).\end{aligned} \tag{3.2}$$

Here, the action of the fourth order elasticity tensor $\mathbb{E}$ is described by $\mathbb{E}\boldsymbol{\tau} = \lambda \operatorname{Tr}\boldsymbol{\tau}\, \mathbf{I}_2 + 2\mu\boldsymbol{\tau}$ for any second order tensor $\boldsymbol{\tau}$, $\lambda > 0$ is the Lamé parameter, $\mu > 0$ is the shear modulus, and $K = \lambda + {}^{2\mu}/_{3}$ is the compressibility modulus of the material. The dual variables $\boldsymbol{\sigma}$ and $\boldsymbol{X}$ can be obtained by deriving the energy density (3.2) with respect to the state variables $\boldsymbol{\varepsilon}$ and $\boldsymbol{p}$:

$$\boldsymbol{\sigma} \coloneqq \frac{\partial \phi}{\partial \boldsymbol{\varepsilon}}(\boldsymbol{\varepsilon}, \boldsymbol{p}) \qquad \text{and} \qquad \boldsymbol{X} \coloneqq -\frac{\partial \phi}{\partial \boldsymbol{p}}(\boldsymbol{\varepsilon}, \boldsymbol{p}). \tag{3.3}$$

In particular, we recall that in this case we simply obtain (2.2).

Now, we introduce some hyperelasticity dependencies in the elasticity tensor, and in particular we suppose $\mathbb{E} = \mathbb{E}(\operatorname{Tr}\boldsymbol{\varepsilon})$. Indeed, as discussed in the previous section, material compliance need to be linear function of strain (2.4). If trace dependence is natural, the deviator one is not obvious as it wouldn't be derivable on hydrostatic axis. Here, in particular, we meet the required conditions by assuming:

$$K(\operatorname{Tr}\boldsymbol{\varepsilon}) = \frac{K_i}{2K_i\beta_m \operatorname{Tr}\boldsymbol{\varepsilon} + 1} \qquad \text{and} \qquad \mu(\operatorname{Tr}\boldsymbol{\varepsilon}) = \frac{\mu_i}{4\mu_i\beta^D \operatorname{Tr}\boldsymbol{\varepsilon} + 1},$$

where $K_i > 0$ and $\mu_i > 0$ are the initial compressibility and shear moduli of the sound material, $\beta_m \geq 0$ and $\beta^D \geq 0$ are the hyperelastic parameters of the model. In addition, we restrict ourselves to the tests in which

$$\operatorname{Tr}\boldsymbol{\varepsilon} > \varepsilon_0 \coloneqq \max\left\{-\frac{1}{2K_i\beta_m}, -\frac{1}{4\mu_i\beta^D}\right\}$$

in order to ensure the positivity of $K_0(\operatorname{Tr}\boldsymbol{\varepsilon})$ and $\mu_0(\operatorname{Tr}\boldsymbol{\varepsilon})$. Denoting with $X_m$ and $\boldsymbol{X}^D$ the spherical and deviatoric components of $\boldsymbol{X}$ as we have done for the stress (3.1), the expression of $\boldsymbol{\sigma}$ and $\boldsymbol{X}$ can be easily obtained thanks to (3.3):

$$\begin{cases} \sigma_m = \dfrac{K_i}{2K_i\beta_m\operatorname{Tr}\boldsymbol{\varepsilon}+1}(\operatorname{Tr}\boldsymbol{\varepsilon}-\operatorname{Tr}\boldsymbol{p}) - \dfrac{K_i^2\beta_m}{(2K_i\beta_m\operatorname{Tr}\boldsymbol{\varepsilon}+1)^2}(\operatorname{Tr}\boldsymbol{\varepsilon}-\operatorname{Tr}\boldsymbol{p})^2 \\ \qquad - \dfrac{4\mu_i^2\beta^D}{(4\mu_i\beta^D\operatorname{Tr}\boldsymbol{\varepsilon}+1)^2}(\boldsymbol{\varepsilon}^D-\boldsymbol{p}^D):(\boldsymbol{\varepsilon}^D-\boldsymbol{p}^D), \\ \boldsymbol{\sigma}^D = \dfrac{2\mu_i}{4\mu_i\beta^D\operatorname{Tr}\boldsymbol{\varepsilon}+1}(\boldsymbol{\varepsilon}^D-\boldsymbol{p}^D), \end{cases} \tag{3.4}$$

and

$$\begin{cases} X_m = \dfrac{K_i}{2K_i\beta_m\operatorname{Tr}\boldsymbol{\varepsilon}+1}(\operatorname{Tr}\boldsymbol{\varepsilon}-\operatorname{Tr}\boldsymbol{p}), \\ \boldsymbol{X}^D = \dfrac{2\mu_i}{4\mu_i\beta^D\operatorname{Tr}\boldsymbol{\varepsilon}+1}(\boldsymbol{\varepsilon}^D-\boldsymbol{p}^D). \end{cases} \tag{3.5}$$

As a consequence, $\boldsymbol{\sigma}$ and $\boldsymbol{X}$ are connected through the following relation:

$$\boldsymbol{\sigma} = \boldsymbol{X} - \left(\beta_m X_m^2 + \beta^D \boldsymbol{X}^D : \boldsymbol{X}^D\right)\mathbf{I}_2. \tag{3.6}$$

Notice that this relation only involves the hyperelastic parameters $\beta_m$ and $\beta^D$.

### 3.3 The plasticity criterion

For our model, we consider the Drucker–Prager criterion in the $\boldsymbol{X}$–space:

$$f_{\boldsymbol{X}}(\boldsymbol{X}) \coloneqq \frac{1}{\sqrt{6}}\left\|\boldsymbol{X}^D\right\| + aX_m - b = 0, \tag{3.7}$$

where $a > 0$ and $b \geq 0$, and we recall that $\|\boldsymbol{\tau}\| \coloneqq \sqrt{\boldsymbol{\tau}:\boldsymbol{\tau}}$. The corresponding elastic domain $\mathbb{K}_{\boldsymbol{X}} \coloneqq \{\boldsymbol{X}^* \in \mathbb{R}^{3\times3}_{\text{sym}} : f_{\boldsymbol{X}}(\boldsymbol{X}^*) \leq 0\}$ is a convex cone with a singular point at $\left(\frac{b}{a}, \mathbf{0}\right)$, and the behavior remains elastic while $f_{\boldsymbol{X}}(\boldsymbol{X}) < 0$. Moreover, consistently with the Standard Generalized Materials framework, we consider an associative model, i.e., we assume that the plasticity evolution follows the normality rule. As a consequence, in the points in which the boundary is smooth, i.e., where the function $f_{\boldsymbol{X}}$ is differentiable, we have

$$\dot{\boldsymbol{p}} = \dot{\lambda}\left(\frac{1}{\sqrt{6}}\frac{\boldsymbol{X}^D}{\|\boldsymbol{X}^D\|} + \frac{a}{3}\mathbf{I}_2\right), \qquad \dot{\lambda} \geq 0. \tag{3.8}$$

For further details, we refer the reader to [24, Section 2]. In addition, if $b \neq 0$, we assume

$$\beta_m \leq \frac{a}{2b}. \tag{3.9}$$

Combining (3.7) with (3.6), one can obtain the explicit expression of the plasticity criterion in the stress space:

$$f_{\boldsymbol{\sigma}}(\boldsymbol{\sigma}) \coloneqq \frac{1}{6}\left(\beta_m + 6a^2\beta^D\right)\left\|\boldsymbol{\sigma}^D\right\|^2 + \frac{1}{\sqrt{6}}\left(a - 2\beta_m b\right)\left\|\boldsymbol{\sigma}^D\right\| + a^2\sigma_m - b\left(a - \beta_m b\right) = 0. \tag{3.10}$$

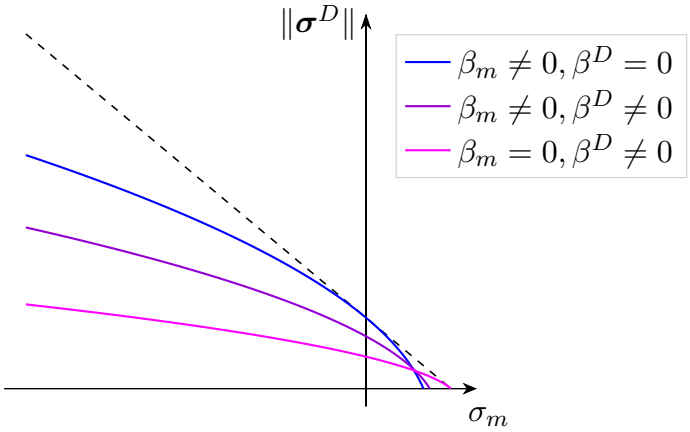


Figure 1: Transformation of the failure criterion for different values of the hyperelastic coefficients $\beta_m$ and $\beta^D$. The black dashed line represents the linear failure criterion (3.7).

Therefore, starting from the linear failure criterion (3.7) for the generalized force $\boldsymbol{X}$, we obtain a quadratic failure criterion for the stress tensor $\boldsymbol{\sigma}$. The corresponding reversibility domain $\mathbb{K}_{\boldsymbol{\sigma}} \coloneqq \{\boldsymbol{\sigma}^* \in \mathbb{R}^{3\times3}_{\text{sym}} : f_{\boldsymbol{\sigma}}(\boldsymbol{\sigma}^*) \leq 0\}$ is a convex cone with parabolic boundary and a singular point in $\left(\frac{b(a-\beta_m b)}{a^2}, \mathbf{0}\right)$. Notice that, since (3.10) does not depend on $\boldsymbol{\varepsilon}$ or $\boldsymbol{p}$, $\mathbb{K}_{\boldsymbol{\sigma}}$ remains fixed for any type of evolution. Figure 1 show the transformation of the failure criterion from linear to quadratic for three different choices of the hyperelasticity parameters $(\beta_m, \beta^D)$.

*Remark* 3.1 (Motivations of assumption (3.9)). Assumption (3.9) ensures that the domain in the stress space is convex and contains the origin $\mathbf{0}$ of the space. Furthermore, with this condition, the quadratic failure criterion can be written as

$$\frac{1}{\sqrt{6}}\|\boldsymbol{\sigma}^D\| = \frac{-(a-2\beta_m b) + a\sqrt{1-4\sigma_m(\beta_m+6a^2\beta^D)+24\beta^D b(a-\beta_m b)}}{2(\beta_m+6a^2\beta^D)}.$$

### 3.4 Implementation considerations

In this section we propose some considerations about the implementation of the constitutive relation determined by (3.4), the plasticity criterion (3.7), and the normal flow rule (3.8).

With the aim of computing the evolution of a material point under the hypothesis of a quasi-static nonlinear problem, we discretize the problem using an incremental approach. For simplicity, for any tensor or scalar variable $x$, its value at the previous equilibrium state, at the current equilibrium state, and its increment are denoted by $x^-$, $x$ and $\Delta x \coloneqq x - x^-$, respectively. Then, in order to solve locally the evolution of a point we have to satisfy the

following equations:

$$\boldsymbol{\sigma} = \mathbb{E}(\operatorname{Tr}\boldsymbol{\varepsilon})(\boldsymbol{\varepsilon}-\boldsymbol{p}) + \frac{1}{2}\frac{\partial \mathbb{E}(\operatorname{Tr}\boldsymbol{\varepsilon})}{\partial \operatorname{Tr}\boldsymbol{\varepsilon}}(\boldsymbol{\varepsilon}-\boldsymbol{p}):(\boldsymbol{\varepsilon}-\boldsymbol{p}), \qquad \text{(definition of } \boldsymbol{\sigma}) \tag{3.11}$$

$$\boldsymbol{X} = \mathbb{E}(\operatorname{Tr}\boldsymbol{\varepsilon})(\boldsymbol{\varepsilon}-\boldsymbol{p}), \qquad \text{(definition of } \boldsymbol{X}) \tag{3.12}$$

$$f_{\boldsymbol{X}}(\boldsymbol{X}) \leq 0, \qquad \text{(yield criterion)} \tag{3.13}$$

$$\Delta\boldsymbol{p} = \Delta\lambda\frac{\partial f_{\boldsymbol{X}}(\boldsymbol{X})}{\partial \boldsymbol{X}}, \Delta\lambda \geq 0, \qquad \text{(flow rule)} \tag{3.14}$$

$$f_{\boldsymbol{X}}(\boldsymbol{X})\Delta\lambda = 0. \qquad \text{(plastic evolution)} \tag{3.15}$$

Here, $\boldsymbol{\varepsilon}$, $\boldsymbol{p}^-$, and, as a consequence, $\boldsymbol{\sigma}^-$ and $\boldsymbol{X}^-$ are known, and the goal is to find the current values $\boldsymbol{p}$, $\boldsymbol{\sigma}$ and $\boldsymbol{X}$. The implementation of this system is composed by two main blocks which correspond to the phase of elastic prediction and to the phase of correction with elasto-plastic evolution.

*Remark* 3.2 (Stress computation). The stress tensor $\boldsymbol{\sigma}$ can be computed directly from $\boldsymbol{X}$ thanks to the relation (3.6), instead of using the explicit expression (3.11). As a consequence, for simplicity, in the following we will only consider (3.12)–(3.15), for which the unknowns are $\Delta\boldsymbol{p}$, $\boldsymbol{X}$, and $\Delta\lambda$.

During the phase of elastic prediction, we define

$$\boldsymbol{X}^{\text{pred}} := \mathbb{E}(\operatorname{Tr}\boldsymbol{\varepsilon})(\boldsymbol{\varepsilon}-\boldsymbol{p}^-).$$

If $f_{\boldsymbol{X}}(\boldsymbol{X}^{\text{pred}}) \leq 0$, then the solution is simply

$$(\Delta\boldsymbol{p}, \boldsymbol{X}, \Delta\lambda) = (\boldsymbol{0}, \boldsymbol{X}^{\text{pred}}, 0).$$

Otherwise, we have to find $(\Delta\boldsymbol{p}, \boldsymbol{X}, \Delta\lambda) \in \mathbb{R}^{3\times3}_{\text{sym}} \times \mathbb{R}^{3\times3}_{\text{sym}} \times \mathbb{R}^+$ such that

$$\begin{cases} \boldsymbol{X} = \mathbb{E}(\operatorname{Tr}\boldsymbol{\varepsilon})(\boldsymbol{\varepsilon}-\boldsymbol{p}^- - \Delta\boldsymbol{p}), \\ \Delta\boldsymbol{p} = \Delta\lambda\dfrac{\partial f_{\boldsymbol{X}}(\boldsymbol{X})}{\partial \boldsymbol{X}}, \\ f_{\boldsymbol{X}}(\boldsymbol{X}) = 0. \end{cases} \tag{3.16}$$

*Remark* 3.3. The system (3.16) with unknowns $(\Delta\boldsymbol{p}, \boldsymbol{X}, \Delta\lambda) \in \mathbb{R}^{3\times3}_{\text{sym}} \times \mathbb{R}^{3\times3}_{\text{sym}} \times \mathbb{R}^+$ has a symmetric jacobian:

$$\tilde{\mathbb{J}} = \begin{pmatrix} \mathbb{E}(\operatorname{Tr}\boldsymbol{\varepsilon}) & \mathbf{I}_4 & \boldsymbol{0} \\ \mathbf{I}_4 & -\Delta\lambda\dfrac{\partial^2 f_{\boldsymbol{X}}(\boldsymbol{X})}{\partial \boldsymbol{X}^2} & -\dfrac{\partial f_{\boldsymbol{X}}(\boldsymbol{X})}{\partial \boldsymbol{X}} \\ \boldsymbol{0} & -\dfrac{\partial f_{\boldsymbol{X}}(\boldsymbol{X})}{\partial \boldsymbol{X}} & 0 \end{pmatrix},$$

where $\mathbf{I}_4$ denotes the fourth order identity tensor. As a consequence, we can easily define an energy function $\tilde{\phi}(\Delta\boldsymbol{p}, \boldsymbol{X}, \Delta\lambda)$ such that solving the problem (3.16) is equivalent to find an extrema of $\tilde{\phi}$. In particular,

$$\tilde{\phi}(\Delta\boldsymbol{p}, \boldsymbol{X}, \Delta\lambda) = \frac{1}{2}\mathbb{E}(\operatorname{Tr}\boldsymbol{\varepsilon})\Delta\boldsymbol{p}:\Delta\boldsymbol{p} + \Delta\boldsymbol{p}:\big(\boldsymbol{X} - \mathbb{E}(\operatorname{Tr}\boldsymbol{\varepsilon})(\boldsymbol{\varepsilon}+\boldsymbol{p}^-)\big) - \Delta\lambda f_{\boldsymbol{X}}(\boldsymbol{X})$$

By defining the elastic part of the strain tensor as $\boldsymbol{\varepsilon}^{\mathrm{el}} \coloneqq \boldsymbol{\varepsilon} - \boldsymbol{p}$, we have

$$\begin{cases} \boldsymbol{X} = \mathbb{E}(\operatorname{Tr}\boldsymbol{\varepsilon})(\boldsymbol{\varepsilon}^{\mathrm{el},-} + \Delta\boldsymbol{\varepsilon}^{\mathrm{el}}), & \text{(3.17a)} \\ \Delta\boldsymbol{\varepsilon}^{\mathrm{el}} = \Delta\boldsymbol{\varepsilon} - \Delta\boldsymbol{p}, & \text{(3.17b)} \\ \Delta\boldsymbol{p} = \Delta\lambda \left( \dfrac{1}{\sqrt{6}} \dfrac{\boldsymbol{\varepsilon}^{\mathrm{el},\mathrm{D},-} + \Delta\boldsymbol{\varepsilon}^{\mathrm{el},\mathrm{D}}}{\|\boldsymbol{\varepsilon}^{\mathrm{el},\mathrm{D},-} + \Delta\boldsymbol{\varepsilon}^{\mathrm{el},\mathrm{D}}\|} + \dfrac{a}{3}\mathbf{I}_2 \right), & \text{(3.17c)} \\ \dfrac{2}{\sqrt{6}}\mu(\operatorname{Tr}\boldsymbol{\varepsilon})\|\boldsymbol{\varepsilon}^{\mathrm{el},\mathrm{D},-} + \Delta\boldsymbol{\varepsilon}^{\mathrm{el},\mathrm{D}}\| + aK(\operatorname{Tr}\boldsymbol{\varepsilon})\operatorname{Tr}(\boldsymbol{\varepsilon}^{\mathrm{el},-} + \Delta\boldsymbol{\varepsilon}^{\mathrm{el}}) - b = 0. & \text{(3.17d)} \end{cases}$$

Notice that the last two equations does not depend explicitly on $\boldsymbol{X}$ anymore, and the latter can be easily computed once we have the increment $\Delta\boldsymbol{\varepsilon}^{\mathrm{el}}$. As a consequence, substituting (3.17c) into (3.17b) the problem is reduced to: Find $(\Delta\boldsymbol{\varepsilon}^{\mathrm{el}}, \Delta\lambda) \in \mathbb{R}^{3\times3}_{\mathrm{sym}} \times \mathbb{R}^{+}$ such that

$$\begin{cases} \Delta\boldsymbol{\varepsilon}^{\mathrm{el}} - \Delta\boldsymbol{\varepsilon} + \Delta\lambda \left( \dfrac{1}{\sqrt{6}} \dfrac{\boldsymbol{\varepsilon}^{\mathrm{el},\mathrm{D},-} + \Delta\boldsymbol{\varepsilon}^{\mathrm{el},\mathrm{D}}}{\|\boldsymbol{\varepsilon}^{\mathrm{el},\mathrm{D},-} + \Delta\boldsymbol{\varepsilon}^{\mathrm{el},\mathrm{D}}\|} + \dfrac{a}{3}\mathbf{I}_2 \right) = \mathbf{0}, \\ \dfrac{2}{\sqrt{6}}\mu(\operatorname{Tr}\boldsymbol{\varepsilon})\|\boldsymbol{\varepsilon}^{\mathrm{el},\mathrm{D},-} + \Delta\boldsymbol{\varepsilon}^{\mathrm{el},\mathrm{D}}\| + aK(\operatorname{Tr}\boldsymbol{\varepsilon})\operatorname{Tr}(\boldsymbol{\varepsilon}^{\mathrm{el},-} + \Delta\boldsymbol{\varepsilon}^{\mathrm{el}}) - b = 0. \end{cases}$$

This nonlinear problem can be solved with some iterative methods like the Newton method, for which we have to compute the Jacobian matrix:

$$\mathbb{J} = \begin{pmatrix} \mathbb{J}_1 & \mathbb{J}_2 \\ \mathbb{J}_3 & 0 \end{pmatrix},$$

where

$$\mathbb{J}_1 \coloneqq \mathbf{I}_4 + \frac{\Delta\lambda}{\sqrt{6}} \left[ \left( \mathbf{I}_4 - \frac{1}{3}\mathbf{I}_2 \otimes \mathbf{I}_2 \right) \frac{1}{\|\boldsymbol{\varepsilon}^{\mathrm{el},\mathrm{D},-} + \Delta\boldsymbol{\varepsilon}^{\mathrm{el},\mathrm{D}}\|} - \frac{(\boldsymbol{\varepsilon}^{\mathrm{el},\mathrm{D},-} + \Delta\boldsymbol{\varepsilon}^{\mathrm{el},\mathrm{D}}) \otimes (\boldsymbol{\varepsilon}^{\mathrm{el},\mathrm{D},-} + \Delta\boldsymbol{\varepsilon}^{\mathrm{el},\mathrm{D}})}{\|\boldsymbol{\varepsilon}^{\mathrm{el},\mathrm{D},-} + \Delta\boldsymbol{\varepsilon}^{\mathrm{el},\mathrm{D}}\|^3} \right],$$

$$\mathbb{J}_2 \coloneqq \frac{1}{\sqrt{6}} \frac{\boldsymbol{\varepsilon}^{\mathrm{el},\mathrm{D},-} + \Delta\boldsymbol{\varepsilon}^{\mathrm{el},\mathrm{D}}}{\|\boldsymbol{\varepsilon}^{\mathrm{el},\mathrm{D},-} + \Delta\boldsymbol{\varepsilon}^{\mathrm{el},\mathrm{D}}\|} + \frac{a}{3}\mathbf{I}_2,$$

$$\mathbb{J}_3 \coloneqq \frac{2}{\sqrt{6}}\mu(\operatorname{Tr}\boldsymbol{\varepsilon}) \frac{\boldsymbol{\varepsilon}^{\mathrm{el},\mathrm{D},-} + \Delta\boldsymbol{\varepsilon}^{\mathrm{el},\mathrm{D}}}{\|\boldsymbol{\varepsilon}^{\mathrm{el},\mathrm{D},-} + \Delta\boldsymbol{\varepsilon}^{\mathrm{el},\mathrm{D}}\|} + aK(\operatorname{Tr}\boldsymbol{\varepsilon})\mathbf{I}_2,$$

and $\otimes$ denotes the tensor product.

# 4 Numerical results

The aim of this section is to show a panel of examples of evolution using the proposed hyperelastic model in some typical test cases. In particular, we want to exhibit the influence of the hyperelastic parameters and to provide a comparison with the linear elasto-plastic model. The results are obtained with the open source code generation tool `mfront` (see [12] and also `http://tfel.sourceforge.net`). For all tests we start from a natural reference configuration with $\boldsymbol{p} = \mathbf{0}$, and we set the Poisson parameter $\nu = 0.3$, which corresponds to the compressibility modulus $K_i = 5E/6$ and to the shear modulus $\mu_i = 5E/13$.

## 4.1 Hydrostatic triaxial tests

During a hydrostatic triaxial test, the stress remains on the hydrostatic axis throughout the loading. This corresponds to the assumption that only the spherical part of the stress

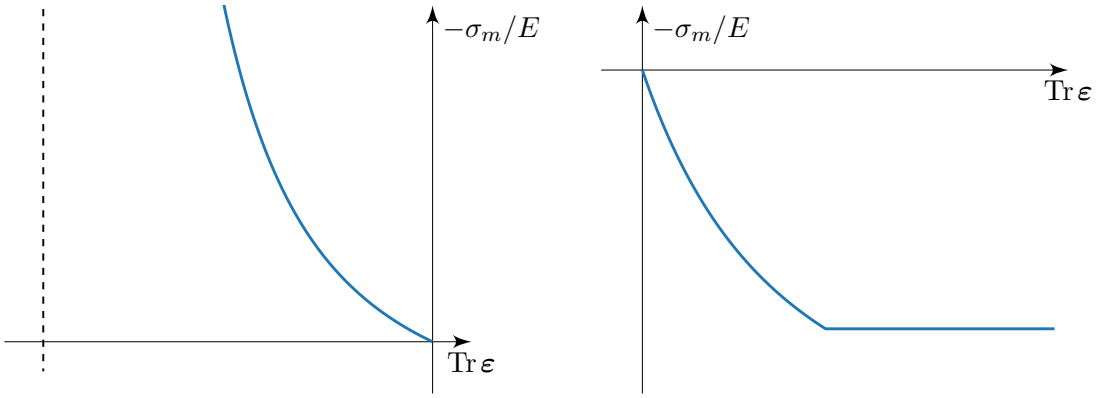


Figure 2: Graphs of hydrostatic triaxial test: compression (*left*) and traction (*right*).

evolves, i.e., $\boldsymbol{\sigma} = \bar{\sigma}\mathbf{I}_2$, with $\bar{\sigma} < 0$ for compression tests, and $\bar{\sigma} > 0$ for traction tests. For simplicity, we suppose that the lower boundary for the evolution of the volumetric part of the strain is $\varepsilon_0 = -\dfrac{1}{2K_i\beta_m}$, i.e., $K_i\beta_m \geq 2\mu_i\beta^D$. From the second equation of (3.4) we have immediately that $\boldsymbol{\varepsilon}^D = \mathbf{0}$. The behavior is always hyperelastic, i.e., $\boldsymbol{\sigma} \in \mathrm{Int}\mathbb{K}_{\boldsymbol{\sigma}}$, during a hydrostatic compression test. In particular, the evolution is simply described by

$$\boldsymbol{\sigma} = \sigma_m\mathbf{I}_2 = \left[\frac{K_i}{2K_i\beta_m\mathrm{Tr}\,\boldsymbol{\varepsilon}+1}\mathrm{Tr}\,\boldsymbol{\varepsilon} - \frac{K_i^2\beta_m}{(2K_i\beta_m\mathrm{Tr}\,\boldsymbol{\varepsilon}+1)^2}(\mathrm{Tr}\,\boldsymbol{\varepsilon})^2\right]\mathbf{I}_2,$$

or

$$\boldsymbol{\varepsilon} = \frac{\mathrm{Tr}\,\boldsymbol{\varepsilon}}{3}\mathbf{I}_2 = \left[\frac{1}{6K_i\beta_m}\left(-1+\frac{1}{\sqrt{1-4\beta_m\sigma_m}}\right)\right]\mathbf{I}_2.$$

In a traction test, there is an initial hyperelastic behavior until $\sigma_m$ reaches his maximum value $\dfrac{b(a-\beta_m b)}{a^2}$ determined by the plasticity criterion (3.10). Then, the spherical part of the stress remains constant and plasticity evolves. One can see the corresponding graphs of the evolution of the hydrostatic stress $\sigma_m$ as function of $\mathrm{Tr}\,\boldsymbol{\varepsilon}$ in Figure 2, in the case of compression (*left*) and traction (*right*) with parameters $a = 1$, $b = E$, $\beta_m = 1/(5E)$, and $\beta^D \leq 13\beta_m/12$.

### 4.2 Uniaxial compression test with a confining pressure

A unilateral compression test with a confining pressure is divided in two phases:

- at first, a hydrostatic compression is performed reaching the value of pressure $p_0$,
- then, we compress along the $z$–axis maintaining the lateral pressure constant.

As we have already seen in the previous subsection, during the confining phase the behavior is elastic, i.e., $\boldsymbol{p} = \mathbf{0}$, and only the hydrostatic component evolves, i.e., $\boldsymbol{\sigma}^D = \boldsymbol{\varepsilon}^D = \mathbf{0}$. At the end of this stage $\boldsymbol{\sigma} = -p_0\,\mathbf{I}_2$ and $\boldsymbol{\varepsilon} = \bar{\varepsilon}\,\mathbf{I}_2$, where $p_0 > 0$ and

$$\bar{\varepsilon} := \frac{1}{6K_i\beta_m}\left(-1+\frac{1}{\sqrt{4\beta_m p_0+1}}\right).$$

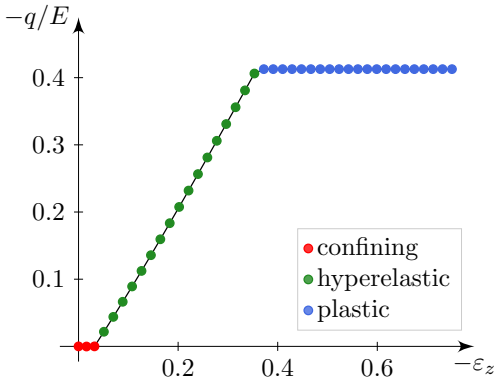


(a) Deviatoric stress $q = \sigma_x - \sigma_z$ vs. axial strain $\varepsilon_z$.

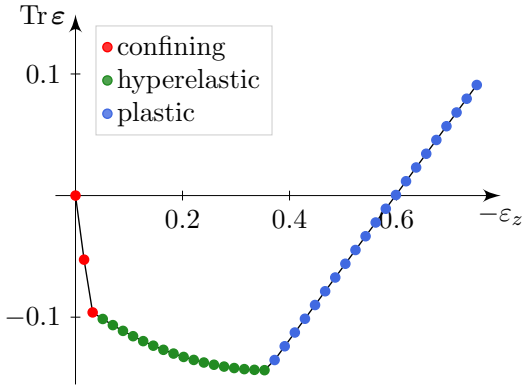


(b) Volumetric strain $\mathrm{Tr}\,\boldsymbol{\varepsilon}$ vs. axial strain $\varepsilon_z$.

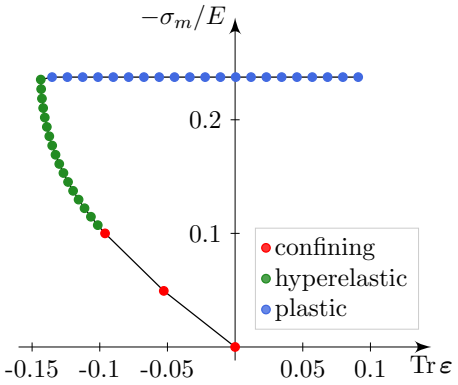


(c) Average stress $\sigma_m$ vs. volumetric strain $\mathrm{Tr}\,\boldsymbol{\varepsilon}$.

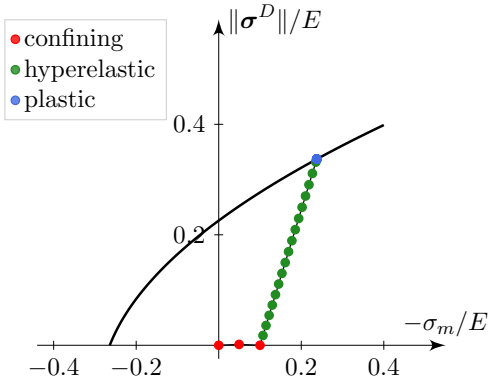


(d) Evolution in the stress domain.

Figure 3: Graphs of uniaxial compression test with a confining pressure. The different stages of the evolution are shown with different colors: hydrostatic confining (*red*), hyperelastic (*green*), and plastic (*blue*) stage.

Then, during the second phase of the loading, we prescribe the evolution of $\varepsilon_z$ with $\dot{\varepsilon}_z < 0$, while the lateral pressure stays equal to $p_0$:

$$\boldsymbol{\sigma} = \begin{pmatrix} -p_0 & 0 & 0 \\ 0 & -p_0 & 0 \\ 0 & 0 & \sigma_z \end{pmatrix} \qquad \text{and} \qquad \boldsymbol{\varepsilon} = \begin{pmatrix} \varepsilon_x & 0 & 0 \\ 0 & \varepsilon_x & 0 \\ 0 & 0 & \varepsilon_z \end{pmatrix}.$$

In addition, in this case we have $\sigma_m = \frac{1}{3}(\sigma_z - 2p_0)$ and $\|\boldsymbol{\sigma}^D\| = \sqrt{\frac{2}{3}}|p_0 + \sigma_z|$, and we define the deviatoric stress $q := p_0 + \sigma_z$. After an initial elastic phase, the boundary of the reversibility domain $\mathbb{K}_{\boldsymbol{\sigma}}$ is reached, and, as a consequence, plasticity starts to evolve following the normality rule.

Figure 3 shows the evolution curves for this kind of test, highlighting with different colors the stages of confining compression, hyperelastic, and plastic evolution. The parameters are given by:

$$a = 0.25, \qquad b = \frac{E}{10}, \qquad \beta_m = \frac{1}{4E}, \qquad \beta^D = \frac{3}{10E}, \qquad p_0 = \frac{E}{10}. \tag{4.1}$$

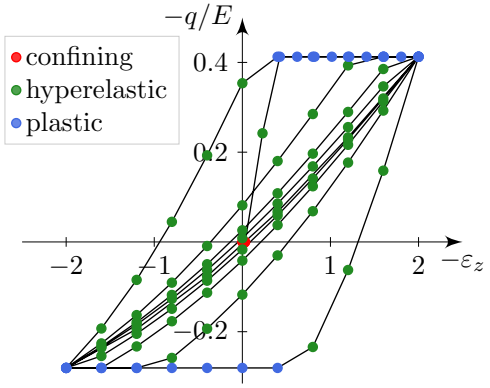


(a) Deviatoric stress $q = \sigma_x - \sigma_z$ vs. axial strain $\varepsilon_z$.

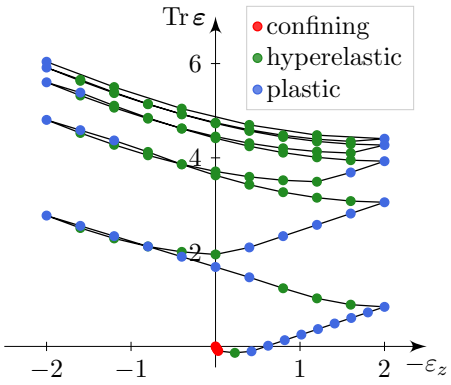


(b) Volumetric strain $\operatorname{Tr}\boldsymbol{\varepsilon}$ vs. axial strain $\varepsilon_z$.

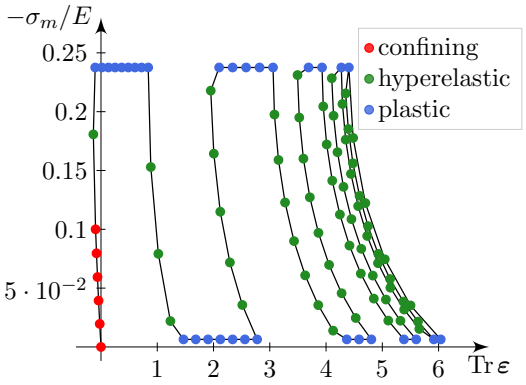


(c) Average stress $\sigma_m$ vs. volumetric strain $\operatorname{Tr}\boldsymbol{\varepsilon}$.

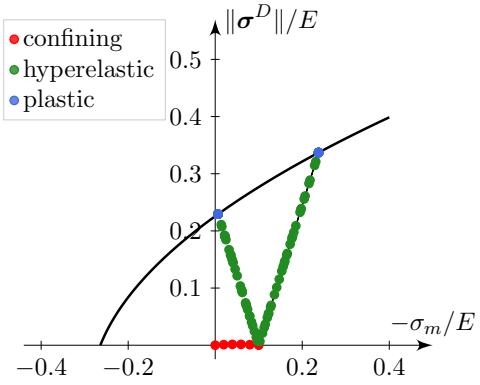


(d) Evolution in the stress domain.

Figure 4: Graphs of cyclic test. The different stages of the evolution are shown with different colors: hydrostatic confining (*red*), hyperelastic (*green*), and plastic (*blue*) stage.

The nonlinear influence is evident especially during the hyperelastic phase (in *green*) in Figures 3b and 3c. During the plastic phase the average stress $\sigma_m$ and the deviatoric stress $q$ stay constant (see Figures 3a and 3c), since in the model we propose the is no hardening coefficient. Moreover, Figure 3b displays the presence of dilatancy without saturation, which is a consequence of the normal flow rule for the evolution of plasticity.

### 4.3 Cyclic test

In this subsection we consider a cyclic test in which at first we perform a hydrostatic compression, and then we decrease and increase cyclically the axial strain $\varepsilon_x$ maintaining the lateral pressure constant. The parameters are again fixed by (4.1). The results are displayed in Figure 4. Notice that the main influence of hyperelasticity is the progressive accomodation of the values. This is particularly relevant for the saturation of dilatancy, Figure 4b.

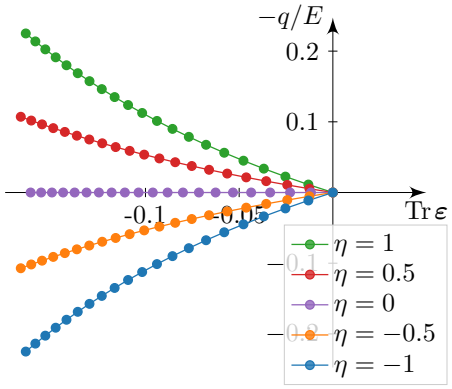


(a) Deviatoric stress $q$ vs. volumetric strain $\operatorname{Tr}\boldsymbol{\varepsilon}$.

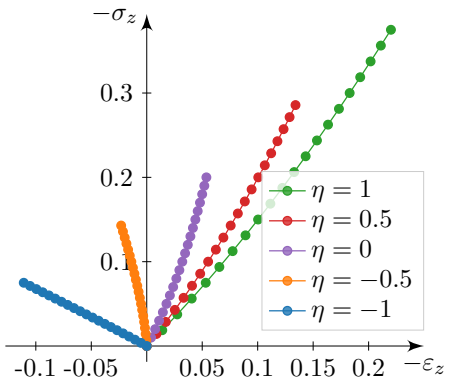


(b) Axial stress $\sigma_z$ vs. axial strain $\varepsilon_z$.

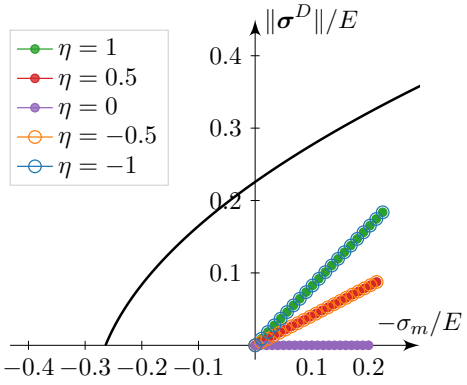


(c) Evolution in the stress domain.

Figure 5: Graphs of radial loadings with different values of $\eta = q/\sigma_m$.

### 4.4 Radial loadings

In this last numerical example, we consider some radial tests, i.e., loadings in which the ratio $\eta := \dfrac{q}{\sigma_m}$ is constant during a compression. Assuming that

$$\boldsymbol{\sigma} = \begin{pmatrix} \sigma_x & 0 & 0 \\ 0 & \sigma_x & 0 \\ 0 & 0 & \sigma_z \end{pmatrix} \qquad \text{and} \qquad \boldsymbol{\varepsilon} = \begin{pmatrix} \varepsilon_x & 0 & 0 \\ 0 & \varepsilon_x & 0 \\ 0 & 0 & \varepsilon_z \end{pmatrix},$$

we have

$$\eta = 3\frac{\sigma_z - \sigma_x}{2\sigma_x + \sigma_z} = \pm\sqrt{\frac{3}{2}}\frac{\|\boldsymbol{\sigma}^D\|}{\sigma_m} = const,$$

which corresponds to

$$\sigma_z = \frac{3 + 2\eta}{3 - \eta}\sigma_x, \qquad \eta \in \mathbb{R}.$$

Figure 5 shows the elastic radial evolution for five different values for $\eta$ and the parameters (4.1). The case $\eta = 0$ (*violet*) corresponds to a hydrostatic compression, i.e., $\|\boldsymbol{\sigma}^D\| = \mathbf{0}$ and $\boldsymbol{\sigma}$ lies on the hydrostatic axis in Figure 5c. For all the other cases, one can notice a nonlinear behavior in the $(q, \operatorname{Tr}\boldsymbol{\varepsilon})$–space, Figure 5a. This kind of behavior can be observed for some geomaterial, we cite for example [23, Figure 9]. In the stress space, the evolution

is linear, Figure 5c, and the angle $\theta$ with the hydrostatic axis depends on the absolute value of $\eta$:

$$\tan\theta = -\sqrt{\frac{2}{3}}|\eta|.$$

# 5 Conclusions

In this paper we have studied the influence of hyperelasticity on the classical perfect plasticity constitutive behavior. It has been shown that, for a particular class of hyperelasticity, the latter phenomenon creates a link between a linear criterion in the generalized force space and a quadratic one in the stress space. On one hand, as first consequence the Hoek–Brown criterion, empirically found long ago, appears to be the natural choice for geomaterials that exhibit nonlinear elastic behavior. On the other hand, the simple fact of observing fixed in stress-space yield surface (independent of plastification level) can point out the hyperbolic elasticity relation, that is easier to fit to experimental data [19]. Furthermore, we have numerically implemented an example of this hyperelasto-plastic model written in the formalism of Standard Generalized Materials. The model has been constructed in the spirit of [8] from an energy function with hyperbolic elastic dependencies in the compressibility and shear moduli. The mechanical properties of the presented model have been investigated in details. Most notably, the obtained model reveals accommodation of dilatancy during uniaxial compression tests with a confining pressure. Being common for many geomaterials and experimentally observed, this saturation of dilatancy constitutes another indirect proof of importance of hyperelasticity. For sure, the simplified example model defined here can hardly represent all aspects of rather complex behavior of real geomaterials. Nevertheless, it can be considered as limiting or initial constitutive relation serving as fundamental brick for more subtle models. The authors foresee some relevant modifications that hyperelasticity would provide for previously proposed damage coupled to plasticity law [24].

# Acknowledgements

The authors would like to thank Goustan Bacquaert, Florian Escoffier and Simon Raude (EDF R&D Palaiseau, France) for numerous fruitful discussions. We thank the CIH team of EDF Hydro (Chambéry, France) for the support and technical advices.

# References

[1] L. R. Alejano and A. Bobet, *Drucker–Prager criterion*, Rock Mechanics and Rock Engineering, 45 (2012), pp. 995–999.

[2] D. Aubry, J. C. Hujeux, F. Lassoudiere, and Y. Meimon, *A double memory model with multiple mechanisms for cyclic soil behavior*, in Proceedings of International Symposium on Numerical Models in Geomechanics, 1982, pp. 3–13.

[3] F. L. L. B. Carneiro, *A new method to determine the tensile strength of concrete*, in Proceedings of the 5th meeting of the Brazilian Association for Technical Rules ("Associação Brasileire de Normas Técnicas—ABNT"), September 1943, pp. 126–129.

[4] C. A. Coulomb, *Essai sur une application des règles des maximis et minimis à quelquels problèmes de statique, relatifs à l'architecture*, Academie Royale Des Sciences Paris Mem. Math. Phys., 7 (1776), pp. 343–382.

[5] Y. F. Dafalias and E. P. Popov, *A model of nonlinearly hardening materials for complex loading*, Acta Mechanica, 21 (1975), pp. 173–192.

[6] D. C. Drucker and W. Prager, *Soil mechanics and plastic analysis or limit design*, Quarterly of Applied Mathematics, 10 (1952), pp. 157–165.

[7] E. Eberhardt, *The Hoek-Brown failure criterion*, Rock Mechanics and Rock Engineering, 45 (2012), pp. 981–988.

[8] I. Einav, G. Houlsby, and G. Nguyen, *Coupled damage and plasticity models derived from energy and dissipation potentials*, International Journal of Solids and Structures, 44 (2007), pp. 2487–2508.

[9] C. Fairhurst, *On the validity of the 'Brazilian' test for brittle materials*, International Journal of Rock Mechanics and Mining Sciences & Geomechanics Abstracts, 1 (1964), pp. 535–546.

[10] A. Griffith, *The theory of rupture*, in Proc. Ist. Int. Congr. Appl. Mech., 1924, pp. 54–63.

[11] B. Halphen and Q. S. Nguyen, *Sur les matériaux standard généralisés*, Journal de Mécanique, 14 (1975), pp. 39–63.

[12] T. Helfer and É. Castelier, *Le générateur de code `mfront`: présentation générale et application aux propriétés matériau et aux modèles*, 2013.

[13] E. Hoek and E. T. Brown, *Empirical strength criterion for rock masses*, Journal of the Geotechnical Engineering Division, 106 (1980), pp. 1013–1035.

[14] E. Hoek and E. T. Brown, *Underground Excavation in Rock*, E & FN Spon, 1982.

[15] ——, *Practical estimates of rock mass strenght*, International Journal of Rock Mechanics and Mining Sciences, 34 (1997), pp. 1165–1186.

[16] ——, *The Hoek–Brown failure criterion and GSI – 2018 edition*, Journal of Rock Mechanics and Geotechnical Engineering, 11 (2019), pp. 445–463.

[17] E. Hoek and P. Marinos, *A brief history of the development of the Hoek–Brown failure criterion*, Solis and Rocks, (2007), pp. 1–13.

[18] C. Jailin, A. Carpiuc, K. Kazymyrenko, M. Poncelet, H. Leclerc, F. Hild, and S. Roux, *Virtual hybrid test control of sinuous crack*, Journal of the Mechanics and Physics of Solids, 102 (2017), pp. 239–256.

[19] L. Knittel, T. Wichtmann, A. Niemunis, G. Huber, E. Espino, and T. Triantafyllidis, *Pure elastic stiffness of sand represented by response envelopes derived from cyclic triaxial tests with local strain measurements*, Acta Geotechnica, 15 (2020), pp. 2075–2088.

[20] J. F. Labuz and A. Zang, *Mohr–Coulomb failure criterion*, Rock Mechanics and Rock Engineering, 45 (2012), pp. 975–979.

[21] S.-K. Lee, Y.-C. Song, and S.-H. Han, *Biaxial behavior of plain concrete of nuclear containment building*, Nuclear Engineering and Design, 227 (2004), pp. 143–153.

[22] H. Li, T. Guo, Y. Nan, and B. Han, *A simplified three-dimensional extension of Hoek–Brown strenght*, Journal of Rock Mechanics and Geotechnical Engineering, 13 (2021), pp. 568–578.

[23] M. P. Luong, *Stress–strain aspects of cohesionless soils under cyclic and transient loading*, in Proceedings of the International Symposium on Soils under Cyclic and Transient Loading, A. A. Balkema, January 1980, pp. 315–324.

[24] J.-J. Marigo and K. Kazymyrenko, *A micromechanical inspired model for the coupled to damage elastoplastic behavior of geomaterials under compression*, Mechanics & Industry, 20 (2019).

[25] O. Mohr, *Welche umstände bedingen die elastizitätsgrenze und den bruch eines materials?*, Zeitschrift des Vereines deutscher Ingenieure, 44 (1900), pp. 1524–1530.

[26] A. Niemunis and M. Cudny, *On hyperelasticity for clays*, Computers and Geotechnics, 23 (1998), pp. 221–236.

[27] R. W. Ogden, *Non-linear elastic deformations*, Ellis Horwood series in mathematics and its applications, E. Horwood Halsted Press, 1984.

[28] X. D. Pan and J. Hudson, *A simplified three-dimensional Hoek-Brown yield criterion*, Proc Symposium on Rock Mechanics and Power Plants, (1988), pp. 95–103.

[29] S. Priest, *Three-dimensional failure criteria based on the Hoek-Brown criterion*, Rock Mechanics and Rock Engineering, 45 (2012), pp. 989–993.

[30] S. Raude, F. Laigle, R. Giot, and R. Fernandes, *A unified thermoplastic/viscoplastic costitutive model for geomaterials*, Acta Geotechnica, 11 (2016), pp. 849–869.

[31] P. A. Veermer and R. de Borst, *Non-associated plasticity for soils, concrete and rock*, vol. 29, 1984.

[32] Q. Zhang, H. Zhu, and L. Zhang, *Modification of a generalized three-dimensional Hoek–Brown strenght criterion*, Internation Journal of Rock Mechanics and Mining Sciences, 59 (2013), pp. 80–96.

[33] Z. Zhou, W. Ma, S. Zhang, Y. Mu, S. Zhao, and G. Li, *Yield surface evolution for columnar ice*, Results in Physics, 6 (2016), pp. 851–859.